MedChemComm

Accepted Manuscript

ROYAL SOCIETY OF CHEMISTRY

www.rsc.org/medchemcomm

Novel pyrrole derivatives as selective CHK1 inhibitors: design, regioselective synthesis and molecular modeling

Taha M. A. Eldebss,[a] Sobhi M. Gomha,[a] and Mohamed M. Abdulla,[b] Reem K. Arafa[c,d*]

[a]*Department of Chemistry, Faculty of Science, Cairo University, Giza 12613, Egypt*

[b]*Research Unit, Saco Pharm. Co., 6th October City, Egypt*

[c]*Pharmaceutical Chemistry Department, Faculty of Pharmacy, Cairo University, 11562Giza, Egypt*

[d]*University of Science and Technology, Zewail City of Science and Technology, 12588 Giza, Egypt*

Abstract

An efficient synthesis of *hitherto* unreported 3-heteroarylpyrroles were described *via* regioselective 1,3-dipolar cycloaddition reactions of enaminones **2** or **3** with nitrilimines **5a-j** to afford the corresponding pyrazole derivatives **7-j.** Hydrazinolysis of the **7a-f** yielded the respective pyrazolo[3,4-*d*]pyridazines **10a-f**. Furthermore, pyrrole analogs substituted on the 3-position with a pyranone (**14**), benzofuran (**16**) or naphthofuran (**18**) were also synthesized. The structures of the synthesized compounds were determined by spectral, elemental analyses and alternative syntheses wherever possible. The synthesized compounds were evaluated for their protein kinases inhibitory activities against 25 kinases belonging to 4 kinase groups *viz.* AGC (5 kinases), CAMK (5 kinases), CMGC (4 kinases) and TK (11 kinases). While the tested compounds were found to be good inhibitors of VEGFR-2 and EGFR, exhibiting low micromolar IC_{50} values, they were selectively more potent against CHK1 eliciting potent inhibitory effect with IC_{50} values in the submicromolar range. Finally, docking studies were performed to interpret the possible binding mode of the target compounds with CHK1.

Keywords: Nitrilimines; 1,3-Dipolar cycloaddition;Pyrazolo[3,4-*d*]pyridazins; VEGFR-2; EGFR and CHK1.

***Corresponding Author.** e-mail address: reem.arafa@pharma.cu.edu.eg;

Tel.: +2 0100-2074028

1. Introduction

Kinases represent a strategic class of enzymes accountable for the regulation of numerous biological functions. Kinases can modulate the function of their targets through covalent attachment of a phosphate group, transferred originally from an ATP molecule, to their target biomolecules, thus leading to a consequent cascade of biological events based on the nature of the phosphorylated client. Although various biomolecules are subject to kinase-mediated phosphorylation (proteins, nucleotides, lipids, etc), protein kinases represent the largest group of kinases, which phosphorylate proteins at key Ser/Thr or Tyr residues. About 2% of the eukaryotes genome encodes for Ser/Thr/Tyr kinases.[1] Ser/Thr/Tyr kinases form a very large protein family. They are divided according to an extended Hanks and Hunter classification into nine main groups which are further subdivided into 81 families and 238 subfamilies corresponding to different substrate specificities and mode of activation.[2-4] Biologically, kinases play a vital rule in cell cycle control, embryonic development, as well as in cancer pathways, hence are valid drug targets for pharmaceutically active molecules aiming to modify any of the aforementioned bio-processes.[5,6]

Design of small-molecule kinase inhibitors as competitors to ATP at its binding site has long been sought by researchers and in fact many are in current clinical use as anticancer agents. Pyrrole-backbone scaffold-containing molecules are among the vast array of compounds found active as PKIs. The well-known multi-target PKIs SU668 and sunitinib (Figure 1) contain a pyrrole functionality as an integral structural motif. Studies on SU6668, initially discovered in 2000,[7] showed that it can inhibit receptor tyrosine phosphorylation and stop mitosis thus suppressing tumor cell proliferation. Consequently, SU6668 was found to elicit a therapeutic effect on a variety of solid tumors and hematological malignancies.[8-10] On the other hand, the multi-kinase inhibitor sunitinib has been approved by the FDA for the management of renal cell carcinoma (RCC) and gastrointestinal stromal tumor (GIST) since 2006 as the first anti-cancer drug to be simultaneously approved for two different indications.[11,12]

An important kinase family member is checkpoint kinase 1 (CHK1) which is a global regulator of the mammalian cell cycle and thus is a valid target for the design of novel anticancer agents. Biologically, CHK1 plays a central role in normal DNA replication, mitosis, and cytokinesis. In addition, CHK1 regulates cell cycle checkpoints upon detection of DNA damage by halting the S or G2/M transition and initiating a DNA-damage response (DDR). Inhibition of CHK1 in the

absence of DNA damage can cause impaired DNA replication, loss of DNA damage checkpoints, premature entry into mitosis, failed metaphase, and cell death *via* mitotic catastrophe.[13,14] Also, inhibition of CHK1 in the presence of DNA damage sensitizes cells to the deleterious effects of genotoxic agents by stalling the DDR. LY2606368 (Figure 1) is a small molecule that *in vitro* preferentially binds to and inhibits CHK1, thus inducing DNA double-strand breaks, a loss in checkpoint function and cell death. It also abrogates DNA-damage initiated DDR.[15] LY2606368 is currently in clinical development as an antitumor agent to be used either as a monotherapy or in combination with genotoxic agents. Additionally, SCH900776 is another potent CHK1 inhibitor that interacts synergistically with DNA antimetabolite agents both *in vitro* and *in vivo* thus selectively inducing dsDNA breaks and cell death in tumor cells (Figure 1).[16] LY2606368 along with SCH900776 both contain a pyrazole ring as a structural backbone unit.

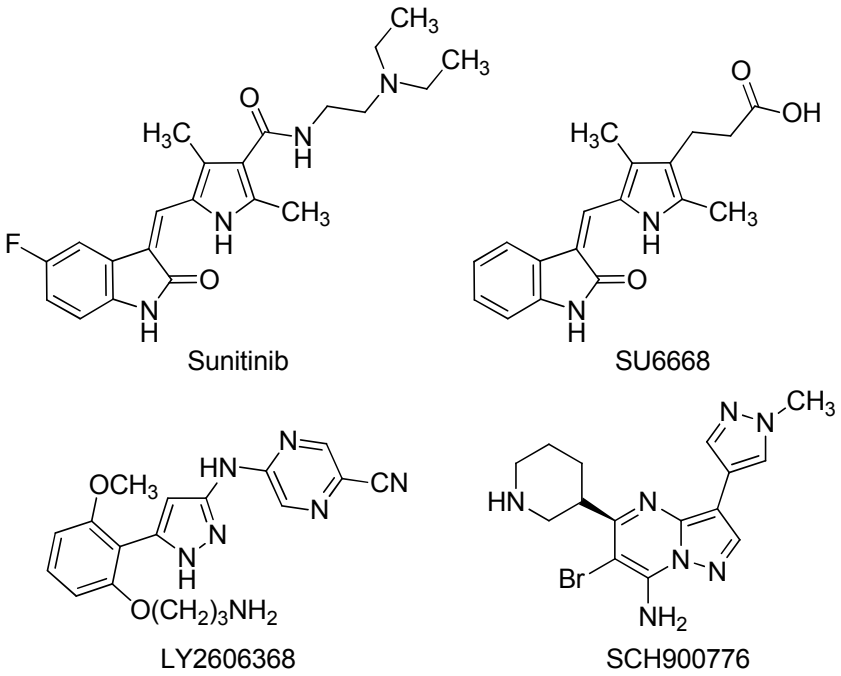

Figure 1. Structures of some pyrrole and pyrazole scaffold-based biologically active PKIs.

In continuation of our previous work aiming at the synthesis of heterocyclic systems with potential activity in cancer management,[17-23] we herein present an efficient regioselective synthesis of novel 3-heteroaryl-pyrroles, which have not been reported *hitherto*. The design strategy of the new compounds was based on decorating the 3-position of the pyrrole ring with substituted pyrazole heterocycles to evaluate the effect of this ring combination in a single molecule on the kinase

inhibitory ability of these chemical entities. Also, bioisosteric replacement of the pyrazole ring with various substituted pyrazolopyridazine moieties was performed with the same objective in mind. Furthermore, structural modification of the pyrazole moiety into a pyranone, benzofuran or naphthofuran heterocyclic counterparts was carried out to study the effect of these structural alterations on the biological activity of this novel series of pyrrole-scaffold based molecules. The target compounds were then screened as PKIs against a panel of 25 PKs representing 4 kinase groups *viz.* AGC (5 kinases), CAMK (5 kinases), CMGC (4 kinases) and TK (11 kinases). The IC_{50} values of the pyrrole-based compounds were determined against the most sensitive kinases in this study vascular endothelial growth factor receptor-2 (VEGFR-2), epidermal growth factor receptor (EGFR) and CHK1 and compounds were found to be more selective to CHK1. Finally, docking protocols were performed to predict the binding modes and affinities of these candidate ligands with CHK1.

2. Results and discussion

2.1. Chemistry

In the course of the current work, and for the exploration of the structure-activity relationship (SAR) of pyrrole-scaffold based molecules as PKIs, we varied the substituents on the 3-position of the pyrrole moiety by the synthesis methods illustrated in Schemes 1 to 4. We have found that the enaminones **2** and **3** were excellent building blocks for the synthesis of a variety of heterocyclic ring systems. The enaminone derivative **2** was obtained from the reaction of 3-acetylpyrrole derivative **1** with dimethylformamide-dimethylacetal (DMF-DMA)[24,25] (Scheme 1). The structure of compound **2** was confirmed by its elemental analysis and spectral data.

Treatment of the enaminone **2** with morpholine under reflux conditions afforded the enaminone **3** (Scheme 1). The IR spectrum of the latter product exhibited a characteristic band at 1669 cm^{-1} corresponding to the carbonyl group. The ^{1}HNMR spectrum of compound **3** revealed five signals corresponding to the CH_3, the two pairs of the equivalent CH_2 groups of the morpholino moiety and the two vinylic CHs at 1.74, 2.92, 3.84, 5.77 and 7.82 ppm, respectively. In addition, displayed in the ^{1}HNMR spectrum of **3** was an aromatic multiplet in the region 7.32–7.61 ppm and a signal at 11.62 ppm (D_2O-exchangeable) characteristic for NH proton**.** Its mass spectrum revealed a peak at m/z 372 corresponding to its molecular ion.

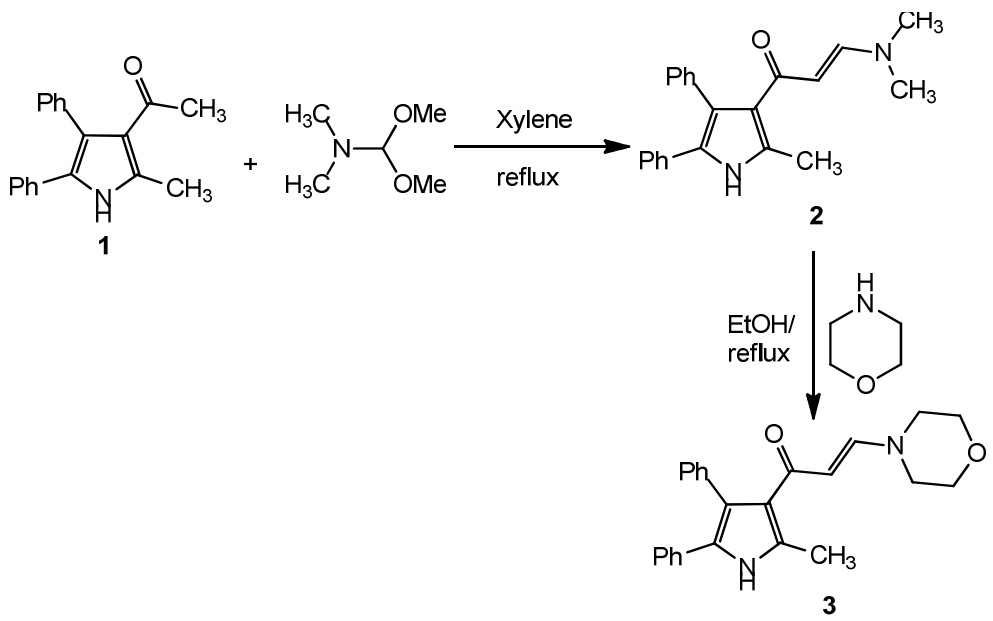

Scheme 1. Synthesis of key synthons **2** and **3**.

When enaminone **2** was allowed to react with the nitrilimines **5a-j** [liberated *in situ* from the corresponding hydrazonyl halides **4a-j**, respectively, upon treatment with triethylamine in refluxing benzene], this afforded the corresponding new pyrazole derivatives **7a-j** (Scheme 2).

For further chemical validation, the nitrilimines **5a-c** were alternatively reacted with the enaminone **3** in refluxing benzene and afforded, in each case, only one isolable product. The reaction products were identified as the pyrazole **7a-c** (Scheme 2), structurally similar to those obtained from the reactions employing **2** as the starting synthon. The latter products were assumed to be formed *via* initial 1,3-dipolar cycloaddition of the nitrilimines **5a-c** to the activated double bond in compound **2** or **3** to afford the non-isolable cycloadducts **6** which underwent loss of dimethylamine or morpholine molecule yielding the final pyrazole derivatives **7a-c.**

The other possible regioisomer **9** was excluded on the basis of the spectral data of the isolated products. It is known that in the pyrazole ring system C-4 is the most electron-rich carbon, thus H-4 is expected to appear in the NMR spectra at higher field, typically near 6.0 ppm. On the other hand, H-5 is linked to the carbon attached to a nitrogen atom and thus it is deshielded to appear near 8.0 ppm. The ^{1}HNMR spectra of the isolated products **7a-c** revealed, in each case a singlet signal in the region of 8.43–8.46 which indicates the presence of the pyrazole H-5 rather than H-4. This conclusion was further confirmed chemically by the reaction compounds **7a-c** with hydrazine hydrate, to afford fused pyrazolopyridazine ring systems **10a-c**, a reaction that would have been

otherwise not possible if products **9a-c** were obtained (Scheme 2). The structures of **10a-c** were confirmed on the basis of their elemental and spectral analys

es. Mainly, the IR spectra of these derivatives showed the disappearance of the two carbonyl bands characteristic for the pyrazoles **7a-c**.

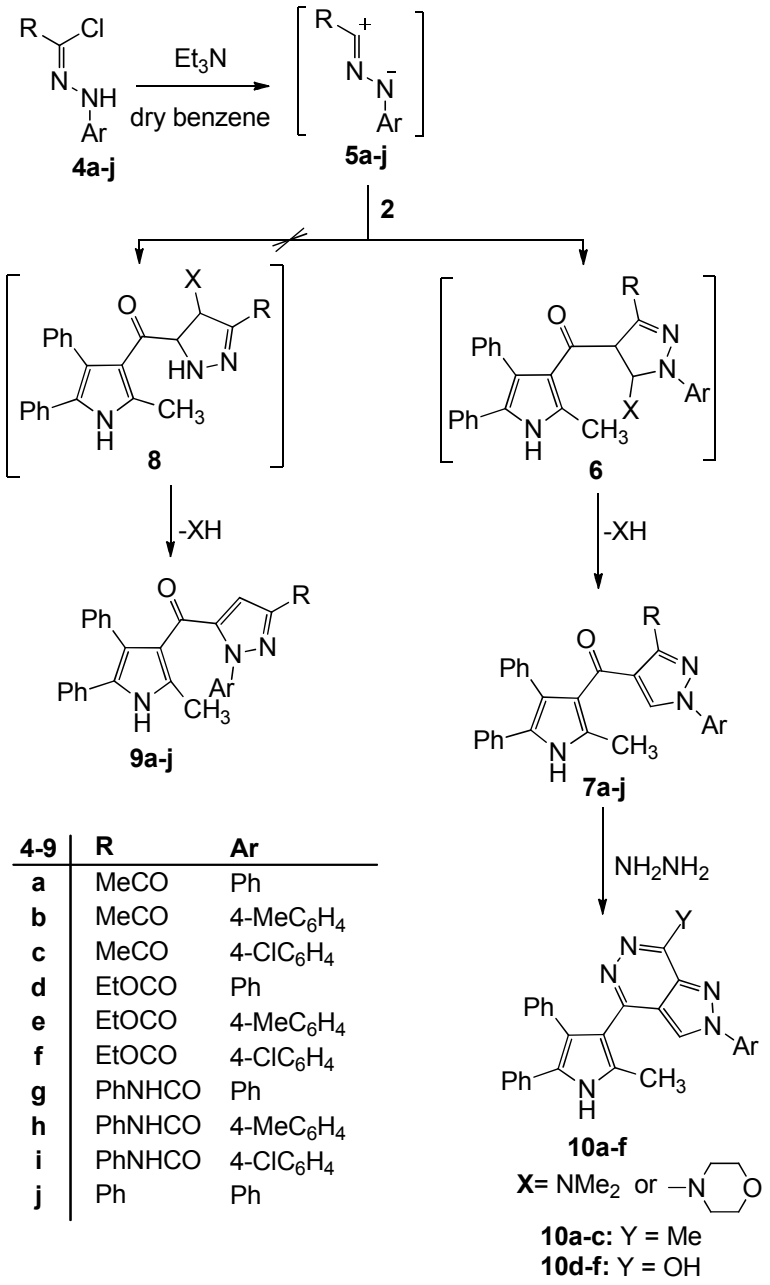

4-9	R	Ar
a	MeCO	Ph
b	MeCO	4-MeC_6H_4
c	MeCO	4-ClC_6H_4
d	EtOCO	Ph
e	EtOCO	4-MeC_6H_4
f	EtOCO	4-ClC_6H_4
g	PhNHCO	Ph
h	PhNHCO	4-MeC_6H_4
i	PhNHCO	4-ClC_6H_4
j	Ph	Ph

Scheme 2. Synthesis of pyrazoles **7a-j** and pyrazolopyridazines **10a-f**.

Similarly, when the enaminone **2** was treated with the nitrilimine **5d-f** they afforded the corresponding pyrazole derivatives **7d-f** (Scheme 2). The structures of the isolated products **7d-f** were established on the basis of their elemental analysis and spectral data. For example, the ^{1}H NMR spectra of compounds **7d-f** displayed, in each case, the pyrazole H-5 in the region of 8.58–8.60 ppm which is in accordance with the proposed structure. Moreover, the IR spectra of the isolated products **7d-f** showed, in each case, two strong absorption bands in the region 1728–1630 cm^{-1} corresponding to two carbonyl groups. A further confirmation of the proposed structure came from the reaction of products **7d-f** with hydrazine hydrate, in refluxing ethanol, which afforded the corresponding fused ring systems **10d-f**. The structures of the products **10d-f** were confirmed on the bases of their elemental analysis and spectral data (see experimental part).

In a similar manner, phenylcarbamolyl-*N*-arylnitrilimines **5g-i** react with the enaminone derivative **2** to furnish the corresponding pyrazole derivatives **20a-c** (Scheme 2).

The IR spectra of the isolated products **7g-i** exhibited, in each case, two strong absorption bands near 1675 and 1634 cm^{-1} corresponding to two carbonyl groups. The ^{1}HNMR spectrum of compound **7g,** taken as a typical exampleof the prepared series, revealed a signal corresponding to the pyrazole H-5 proton at 8.48 ppm, in addition to an aromatic multiplet in the region 7.16-7.49 ppm and a singlet signal at 11.91 ppm (D_2O-exchangeable) characteristic for the NH proton.

Similarly, when the enaminone **2** or **3** was treated with nitrileimine **5j**, it afforded pyrazole derivative **7j** (Scheme 2).

Compound **7j** was supported by an alternate chemical synthesis *via* the reaction of the morpholinyl enminone **3** with nitrileimine **5j** (Scheme 2). The product obtained from this reaction was similar in all spectral and elemental aspects with that obtained from the reaction of **2** with **5j** and identified as the pyrazole derivative **7j** (See experimental part).

Treatment of the enaminone **2** or **3** with hippuric acid in refluxing acetic anhydride led to the formation of pyranone derivative **14**. The structure of the latter compound was confirmed on the basis of its elemental analysis and spectral data as detailed in the experimental part. Compound **14** was assumed to be formed *via* the reaction of the intermediate oxazolone **12** (formed *in situ*) with the enaminone **2** or **3**, yielding the non-isolable intermediate **13**, that further rearranged into the pyranone derivative **14** (Scheme 3).

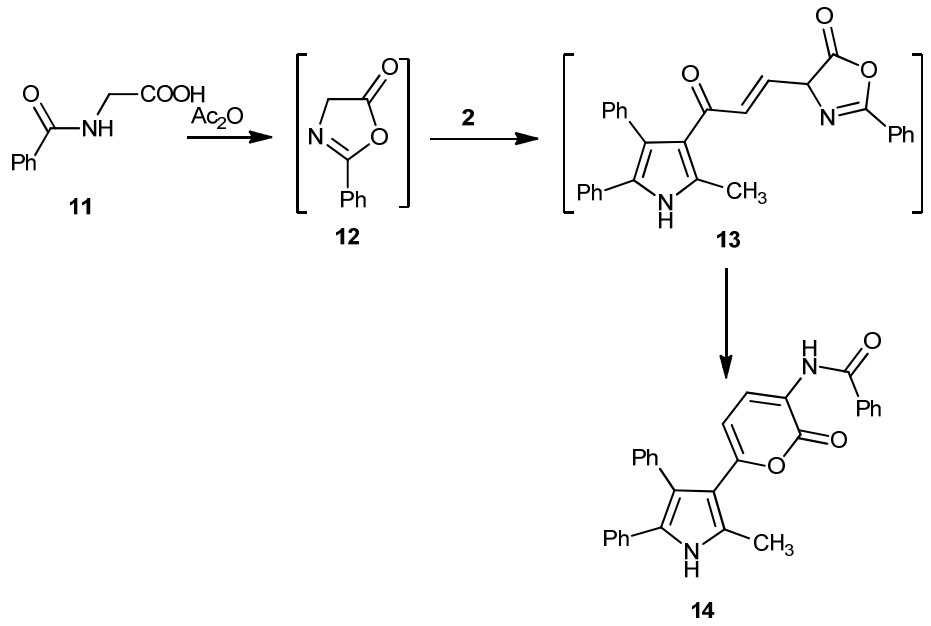

Scheme 3. Synthesis of pyranone derivative **14**.

The reaction of either the enaminone **2** or **3** with p-benzoquinone (**15)** in acetic acid at room temperature, yielded a single product assigned as (5-hydroxybenzofuran-3-yl)(2-methyl-4,5-diphenyl-1*H*-pyrrol-3-yl)methanone (**16**). The mechanism of formation of **16** was proposed to proceed *via* initial addition of the electron-rich moiety C2 in the enaminone **2** or **3** to the activated electron-poor double bond system in the quinone to afford the target compound [26, 27] (Scheme 4). Similarly, the reaction of 1,4-naphthoquinone (**17)** with the enaminone **2** or **3** afforded **18** (Scheme 4). This proposed reaction sequence is analogous to the Nenitzescu reaction of quinones with enaminones. [28]

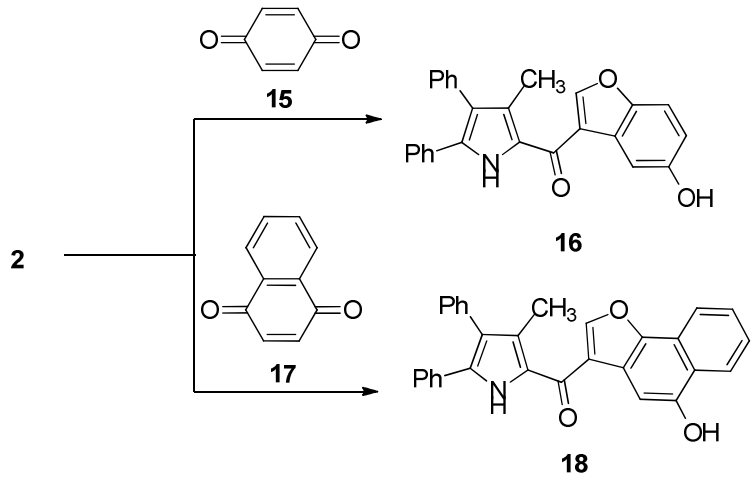

Scheme 4. Synthesis of compounds **16** and **18**.

2.2. Kinase inhibition assay and SAR findings

The newly synthesized compounds were tested for protein kinase inhibition in a panel of 25 enzymes belonging to 4 kinome families *viz.* AGC (5 kinases), CAMK (5 kinases), CMGC (4 kinases) and TK (11 kinases) using a commercially available microfluidic assay format.[29, 30] The inhibitors were tested at a concentration of 30 μM, so that significant activity (> 50 % inhibition) would be indicative of ligand efficient binding (> 0.3 $Kcal^{-1}HA^{-1}$).[31] The ATP concentration used was approximately the Km, [ATP] for each enzyme tested. [32] The % kinase activity inhibition was first determined for all the tested compounds against the full panel of the 25 kinases at a single fixed high concentration. While all the kinases showed variable degrees of response to the inhibition caused by the tested novel pyrrole derivatives, only 3 kinases were highly inhibited by all members of this series of compounds (Table 1). It was found that the most responsive kinases were VEGFR-2 and EGFR from the TK family with all compounds causing 100% enzyme activity inhibition against both enzymes. Also, the tested compounds caused lowering of CHK1 kinase, belonging to the CAMK family, in the range of 76–100%.

Table 1: Heat map showing the % kinase activity inhibition against a panel of 25 kinases by the new pyrrole derivatives tested at 30 μM.

Kinase family	Kinase	Compound #																		
		7a	**7b**	**7c**	**7d**	**7e**	**7f**	**7g**	**7h**	**7i**	**7j**	**10a**	**10b**	**10c**	**10d**	**10e**	**10f**	**14**	**16**	**18**
AGC	**AKT1**	5	7	6	35	46	7	45	12	3	24	12	56	42	90	78	65	32	12	13
	AKT2	3	2	4	36	34	8	86	44	69	32	21	32	35	56	44	58	45	32	56
	MSK1	5	5	4	4	35	45	87	90	56	87	12	7	56	34	65	23	54	32	34
	RSK1	23	13	12	38	3	33	2	4	35	25	17	14	16	36	9	25	34	3	4
	PKC	33	34	45	12	36	23	44	58	36	67	13	35	24	63	47	84	65	32	34
CAMK	**MK2**	2	45	33	57	35	88	26	45	15	34	37	24	26	19	10	18	23	56	76
	MAPKAPK5	43	65	45	54	34	98	54	34	56	56	56	43	46	32	34	34	43	56	54
	PKD2	23	23	43	56	78	98	65	65	67	54	54	45	67	32	64	45	68	76	54
	CHK1	100	90	100	85	82	89	80	81	89	78	83	76	89	84	83	87	80	90	96
	CHK2	34	32	22	46	12	65	4	3	32	54	35	12	24	24	23	34	64	7	55
CMGC	**Erk1**	3	3	45	7	5	7	8	6	7	7	6	2	5	8	7	9	5	4	3
	Erk2	21	22	23	32	32	3	24	34	23	35	32	21	24	23	12	21	4	3	21
	GSK3	12	32	21	13	4	4	23	43	11	3	2	32	12	43	5	32	2	3	2
	p38a	3	3	2	2	3	22	13	12	21	12	4	4	3	2	1	12	32	24	21
TK	**ABL**	2	4	3	2	3	44	32	34	32	3	1	3	2	5	4	44	2	3	4
	FYN	2	11	23	21	21	5	21	23	23	21	12	12	12	12	13	12	21	23	21
	InsR	2	2	3	2	33	8	33	44	12	4	1	3	2	12	22	12	3	2	32
	LYN	3	2	3	5	4	9	24	31	34	24	3	2	4	5	3	54	33	21	34
	LCK	22	21	32	23	23	21	25	46	34	44	43	43	45	32	34	34	34	32	32
	MET	32	2	33	6	56	32	3	22	45	45	5	3	4	4	33	33	22	32	34
	SRC	21	23	22	23	21	12	33	12	21	12	43	11	22	23	21	21	12	32	21
	CK1d	2	4	33	34	32	24	43	44	32	33	24	2	33	53	3	44	24	32	22
	AurA	8	11	1	24	13	12	2	12	3	12	32	12	12	32	32	4	12	12	23
	VEGFR-2	100	100	100	100	100	100	100	100	100	100	100	100	100	100	100	100	100	100	100
	EGFR	100	100	100	100	100	100	100	100	100	100	100	100	100	100	100	100	100	100	100

Since, the non-linear relationship between % inhibition and concentration does not permit differentiation between compounds with similar high % inhibitions (e.g., between 95–100%), even though there may be significant differences in the IC_{50}, and thus selectivity cannot be accurately quantified.[33-35] Thus, full IC_{50} for each compound against VEGFR-2, EGFR and CHK1 was

determined (Table 2) and SAR conclusions drawn from the results of the IC_{50} determination assays against VEGFR-2, EGFR and CHK1 are designated below.

Table 2: IC_{50} determination of enzyme inhibition against VEGFR-2, EGFR and CHK1 by the new pyrrole derivatives.

Compd. #	Enzyme inhibition (IC_{50}/μM)*			Selectivity index**	
	VEGFR-2	EGFR	CHK1	$SI_{VEGFR-2}$	SI_{EGFR}
7a	4.49	4.67	0.12	37.41	38.91
7b	8.77	9.19	0.31	28.29	29.64
7c	4.34	4.48	0.21	20.66	21.33
7d	2.34	3.22	0.67	3.49	4.80
7e	7.56	7.88	0.77	9.81	10.23
7f	2.87	3.2	0.53	5.41	6.03
7g	3.45	3.56	0.80	4.31	4.45
7h	4.33	4.49	0.80	5.41	5.61
7i	3.49	3.78	0.51	6.84	7.41
7j	2.34	2.56	0.91	2.57	2.81
10a	3.45	3.89	0.70	4.92	5.55
10b	4.36	5.43	0.99	4.40	5.48
10c	2.39	2.55	0.54	4.42	4.71
10d	3.45	3.6	0.69	5.00	5.21
10e	3.22	3.45	0.75	4.29	4.6
10f	3.45	4.39	0.56	6.16	7.83
14	2.45	2.89	0.78	3.14	3.70
16	3.45	3.67	0.45	7.66	8.15
18	4.56	5.1	0.31	14.70	16.45

* IC_{50} values are the average of at least 3 experiments.
** Selectivity indices were calculated by using the following formulae: $SI_{VEGFR-2} = IC_{50}$ VEGFR-2/IC_{50} CHK1; $SI_{EGFR} = IC_{50}$ EGFR/IC_{50} CHK1

With respect to the VEGFR-2 inhibition assay, all compounds elicited moderate kinase activity inhibition with IC_{50} values in the range of 2.34-8.77 μM. Regarding the SAR findings of the

pyrazole analogs *viz.* **7a-c** (3-acetyl derivatives), **7d-f** (3-ethoxycarbonyl derivatives), **7g-i** (3-(N-phenyl)carboxamide derivatives) and **7j** (3-phenyl derivative), it was found that the most active members in this set of compounds are **7d** and **7j** with equal IC_{50} of 2.34 µM followed by **7f** (IC_{50} of 2.87 µM). Furthermore, it was found that the 3-ethoxycarbonyl derivatives **15a-c** were more potent than the other pyrazole analogs **7a-c** and **7g-i**. Within each set of pyrazole derivatives, it was found that those compounds bearing a 4-chlorophenyl substituent on the 1-position of the pyrazole ring (**7b**, **7e** and **7h;** IC_{50} values = 8.77, 7.46 and 4.33 µM, respectively) were always less potent than their respective counterparts carrying either a phenyl or a 4-methylphenyl ring (**7a**&**c**, **7d**&**f** and **7g**&**i**).

On the other hand, the pyrazolopyridazine derivatives **10a-c** and **10d-f** were obtained from their respective pyrazole precursors **7a-c** and **7d-f** to study the effect of introduction of a bicyclic heterocyclic system on the 3-position of the pyrrole ring on the biological activity of this class of compounds. While the methylpyrazolopyridazine derivatives **10a-c** elicited an improved VEGFR-2 activity compared to their synthesis precursors **7a-c**, the hydroxypyrazolopyridazines **10d-f** were less potent than their originators **7d-f** with the only exception being **10e** (IC_{50} = 3.22 µM) which was over two folds more potent than the **7e** (IC_{50} = 7.56 µM). Furthermore, the pyrrole derivative with a pyranone side chain **14** showed high potency relative to the other tested compounds (IC_{50} = 2.45 µM). Finally, regarding the benzofuran derivative **16** (IC_{50} = 3.45 µM) and its naphthofuran analog **18** (IC_{50} = 4.56 µM), both compounds were moderately active VEGFR-2 inhibitors with potency favoring the analog with the less bulky side chain.

Moreover, as regards the EGFR kinase inhibition assay, all compounds were moderately potent showing IC_{50} values in the micromolar range and followed a similar SAR behavior as that displayed in the VEGFR-2 inhibition assay. The most potent compounds in this assay were **10c**, **7j** and **14** with IC_{50} values of 2.55, 2.56 and 2.89 µM, respectively.

On the other hand, all the tested compounds were highly potent and more selective CHK1 inhibitors eliciting IC_{50} values in the submicromolar range. The most effective CHK1 inhibitory activity in this series was achieved by the 3-acetylpyrazoles **7a-c** (IC_{50} values of 0.12, 0.31 and 0.21 µM, respectively). With respect to the 3-ethoxycarbonylpyrazole analogs **15a-c** and the 3-(N-phenyl)carboxamide counterparts **7g-i**, though they showed high CHK1 inhibitory efficacy (IC_{50} range from 0.51 to 0.80 µM), they were at least 1.6 fold less potent than their 3-acetyl bioisosteres **7a-c**. With regards to them ethylpyrazolopyridazine derivatives **10a-c** and their hydroxypyrazolopyridazine bioisosteres **10d-f**, the analogous pairs from both series, **10a** and **10d**

as well as **10c** and **10f**, were almost equipotent CHK1 inhibitors, yet the pair **10b** and **10e** showed significantly different CHK1 inhibitory power (IC_{50} = 0.99 and 0.75 μM, respectively). It is noteworthy that synthetic transformation of the 3-acetylpyrazoles **7a-c** (IC_{50} values of 0.12, 0.31 and 0.21 μM, respectively) to the methylpyrazolopyridazines **10a-c** (IC_{50} values of 0.70, 0.99 and 0.54 μM, respectively) significantly reduced the CHK1 inhibition ability of the latter by at least 2.6 fold. However, preparation of the hydroxypyrazolopyridazine derivatives **10d-f** (IC_{50} values of 0.69, 0.75 and 0.56 μM, respectively) from their synthesis precursors **7d-f** (IC_{50} values of 0.67, 0.77 and 0.53 μM, respectively) did not significantly alter the biological activity of the latter. Finally, the potency of the pyrrole derivatives with pyranone **14**, benzofuran **16** and naphthofuran **18** side chain was in increasing order from the smaller side chain to the larger one (IC_{50} values of 0.78, 0.45 and 0.31 μM, respectively) indicating that bulkiness is well tolerated and in fact is favored for enhancing the CHK1 inhibitory activity of these compounds.

Finally, to determine selectivity of these novel pyrrole-scaffold based derivatives, the selectivity index (SI) of these compounds towards CHK1 was calculated relative to both VEGFR-2 ($SI_{VEGFR-2}$) and EGFR (SI_{EGFR}) (table 2). All tested derivatives were CHK1 selective displaying $SI_{VEGFR-2}$ values in the range of 2.57-37.41 and SI_{EGFR} between 2.81 and 38.91. The highest SI values were demonstrated by the acetylpyrazole derivatives **7a-c** being at least 20 fold more selective to CHK1. In compliance with the observed enzyme assay findings, **7a** was the most selective member of this series of kinase inhibitors. Additionally, high selectivity was displayed by the naphthofuran derivative **18** ($SI_{VEGFR-2}$ = 14.70 and SI_{EGFR} = 16.45) and the ethoxycarbonylpyrazole **7e** ($SI_{VEGFR-2}$ = 9.81 and SI_{EGFR} = 10.23). Finally, all other synthesized compounds showed variable degrees of selectivity towards CHK1. The CHK1 selectivity elicited by these compounds gives them an advantage over clinically used multi-kinase inhibitors as they will lack the untoward side effects usually associated with interaction with off-target biomolecules.

2.3. Molecular modeling and docking results

Based on the very interesting CHK1 inhibition assay results, the goal of this part of the study was to attempt to better understand the underlying molecular basis of the observed enzyme inhibition. Thus, a docking experiment was performed to simulate the possible binding mode and affinity of this new series of candidate ligands with CHK1 active site amino acids. CHK1 protein structure obtained from the protein databank (PDB ID: 2YRX)[36] was chosen for this purpose utilizing the MOE v10.2008 software. After protein preparation using the standard procedure and to initially

validate the docking procedure, the native co-crystallized ligand was re-docked in the active site of CHK1. The validation results showed that the docking procedure was able to correctly place the native ligand in the active site as reflected through the obtained rmsd which was equal to 0.2298. The native ligand, CHK1 IC_{50} = 0.02 µM,[36] was bound to the active site amino acids with four hydrogen bonds *viz.* one bond with Glu85 (2.80 Å), one with Glu91 (2.40 Å) and two with Cys87 (2.60 and 2.70 Å) with a binding energy score of S = –18.3042 Kcal.mol^{-1} (data not shown).

After preparing the compounds for docking as explained in the experimental section, they were individually docked with CHK1 and the modes and affinities of their binding interactions were investigated. Indeed, all members of this class of pyrrole derivatives were able to recognize the active site of CHK1 and form hydrogen bonds with key active site amino acid residues (data not shown). As a representative of the obtained docking results, 2D and 3D binding interactions of **7a**, the most active CHK1 inhibitor in this study with an IC_{50} of 0.12 µM, are displayed in the left and right panels of Figure 2, respectively. Docking results showed that **7a** was able to recognize, fit in the active pocket of CHK1 and bind with its key amino acid residues in a fashion similar to the native ligand (Figure 2, right panel). The derivative **7a** interacts with CHK1 through two hydrogen, one between the pyrrole NH and Glu91 (2.50 Å) and another between the oxygen atom of the acetyl side chain and Cys87 (2.80 Å) and a pi-cationic interaction between the phenyl ring at position 4 of the pyrrole and Lys38 as depicted in Figure 2.

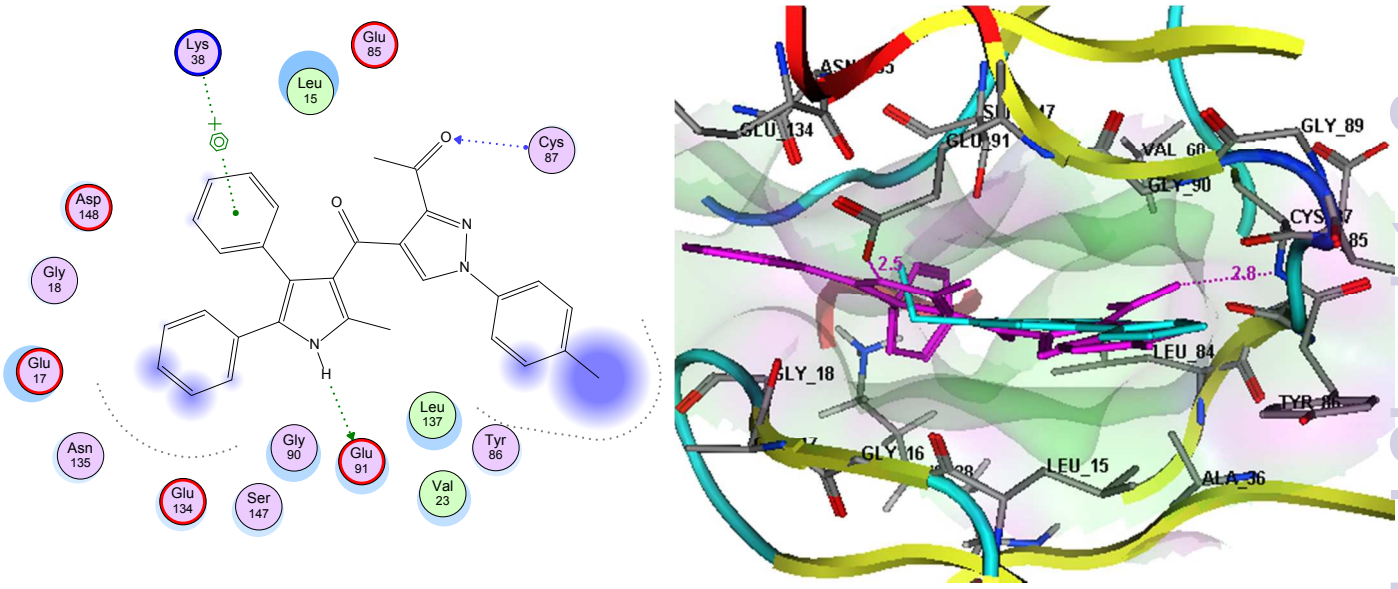

Figure 2. 2D binding interactions of **7a** with active site amino acids of CHK1 (left panel); 3D binding interactions of **7a** (magenta-colored carbons) and the native ligand (cyan-colored carbons) with the active site amino acids of CHK1, hydrogen bonds are shown as orange lines (right panel).

3. Conclusions

The synthetic potential of 3-(dimethylamino)-1-(2-methyl-4,5-diphenyl-1*H*-pyrrol-3-yl)prop-2-en-1-one (**2**) or 1-(2-methyl-4,5-diphenyl-1*H*-pyrrol-3-yl)-3-morpholinoprop-2-en-1-one (**3**) as a versatile, readily accessible building unit for the synthesis of new heterocyclic-substituted pyrroles of biological and pharmacological importance was explored. Thus, **2** or **3** were reacted with nitrilimines **5a-j** to afford the corresponding pyrazole derivatives **7a-j**. Hydrazinolysis of the **7a-f** yielded the respective 4-(pyrrol-3-yl)-2*H*-pyrazolo[3,4-*d*]pyridazines **10a-f**. The synthesized compounds were evaluated at an initial single high dose (30 μM) against a panel of 25 kinases to assess their % kinase activity inhibition. It was found that the most responsive kinases to this series of compounds were VEGFR-2, EGFR and CHK1. Accordingly, the IC_{50} values of these candidate kinase inhibitors were determined against the three aforementioned kinase. The results revealed that all the tested compounds were good inhibitors to VEGFR-2 and EGFR (low micromolar IC_{50} values). Yet, they were more potent and selective inhibitors against CHK1 (submicromolar IC_{50} values). The most potent CHK1 inhibitor in this study was **7a** with IC_{50} = 0.12 μM and also elicited the best selectivity against VEGFR-2 and EGFR with SI indices of 37.41 and 38.91, respectively. Docking studies showed that these compounds fit nicely in the active pocket of CHK1 being able to form hydrogen bonding interactions with key active site amino acid residues. In conclusion, this class of molecules, especially **7a-c**, represent interesting leads for the design and synthesis of selective CHK1 inhibitors.

References

1. Krupa, A.; Abhinandan, K.; Srinivasan, N. *J. Nucleic Acids Res*.**2004**, *32*, D153-D155.
2. Martin, D. M.; Miranda-Saavedra, D.; Barton, G. *J. Nucleic Acids Res*. **2009**, *37*, D244-D250.
3. Smith, C. M.; Shindyalov, I. N.; Veretnik, S.; Gribskov, M.; Taylor, S. S.; Ten Eyck, L. F. Bourne, P. *Trends Biochem. Sci.***1997**, *22*, 444-446.
4. Niedner, R. H.; Buzko, O. V.; Haste, N. M.; Taylor, A.; Gribskov, M.; Taylor, S. S. *Proteins* **2006**, *63*, 78-86.
5. Cohen, P. *Nat. Rev. Drug Discov.***2002**, *1*, 309-315.
6. Han, E.; McGonigal, T. *Anticancer Agents Med. Chem*. **2007**, *7*, 681-684.

7. Laird, A. D.; Vajkoczy, P.; Shawver, L. K.; Thurnher, A.; Liang, C.; Mohammadi, M.; Schlessinger, J.; Ullrich, A.; Hubbard, S. R.; Blake, R. A.; Fong, T. A.; Strawn, L. M.; Sun, L.; Tang, C.; Hawtin, R.; Tang, F.; Shenoy, N.; Hirth, K. P.; McMahon, G.; Cherrington, J. M. *Cancer Res.* **2000**, *60*, 4152-4160.
8. Sessa, C.; Viganò, L.; Grasselli, G.; Trigo, J.; Marimon, I.; Lladò, A.; Locatelli, A.; Ielmini, N.; Marsoni, S.; Gianni, L**.** *Eur. J. Cancer* **2006**, *42*, 171-178.
9. Grosicki, S.; Grosicka, A.; Holowiecki, J. *Wiad. Lek*. **2007**, *60*, 39-46.
10. Van, T. T.; Hanibuchi, M.; Goto, H.; Kuramoto, T.; Yukishige, S.; Kakiuchi, S.; Sato, S.; Sakaguchi, S.; Dat, T.; Nishioka, le Y.; Akiyama, S.; Sone, S. *Respirology,***2012**, *17*,984-504.
11. Demetri, G. D.; vanOosterom, A. T.; Garrett, C. R.; Blackstein, M. E.; Shah, M. H.; Verweij, J.; McArthur, G.; Judson, I. R.; Heinrich, M. C.; Morgan, J. A.; Desai, J.; Fletcher, C. D.; George, S.; Bello, C. L.; Huang, X.; Baum, C. M. Casali, P. G. *Lancet*, **2006**, 368, 1329-1338.
12. Chiang, C.; Lin, Y.; Lin, S.; Lai, C.; Liu, C.; Wei, W.; Yang, S.; Wang, R.; Teng, L.; Chuang, S.; Chang, J.; Yuan, T.; Lee, Y.; Chen, P.; Chi, W.; Yang, J.; Huang, H.; Liao, C.; Huang, J. *J. Med. Chem*. **2010**, *53*, 5929-5941.
13. Thompson, R.; Eastman, A. *Br. J. Clin. Pharmacol*. **2013**, *76*, 358-369.
14. Bucher, N.; Britten, C. D. *Br. J. Cancer*. **2008**, *98*, 523-528.
15. Marshall, M.; Barnard, D.; Diaz, B. EORTC-NCI-AACR Symposium on Molecular Targets and Cancer Therapeutics; November 16-19, 2010; Berlin, Germany. Abstract 194.
16. Guzi, T. J.; Paruch, K.; Dwyer, M. P.; Labroli, M.; Shanahan, F.; Davis, N.; Taricani, L.;Wiswell, D.; Seghezzi, W.; Penaflor, E.; Bhagwat, B.; Wang, W.; Gu, D.; Hsieh, Y.; Lee, S.; Liu, M.; Parry, D. *Mol. Cancer Ther.* **2011**, *10*, 591-602.
17. Farag, A. M.; Ali, K. A.; El-Debss, T. M. A.; Mayhoub, A.S.; Amr, A. E.; Abdel-Hafez, N. A.; Abdulla, M. M. *Eur. J. Med. Chem*. **2010**, *45*, 5887-5898.
18. Gomha, S. M.; Eldebss, T. M. A.; Abdulla, M. M.; Mayhoub, A. S. *Eur. J. Med. Chem*. **2014**, *82*, 472-479.
19. Gomha, S. M.; Riyadh, S. M.; Abbas, I. M.; Bauomi, M. A. *Heterocycles* **2013**, *87*, 341-356.
20. Badrey, M. G.; Gomha, S. M. *Molecules* **2012**, 17, 11538-11553.
21. Gomha, S. M.; Salah, T.A.; Abdelhamid, A. O. *Monatsh. Chem.* **2015**, *146*, 149-158.
22. Gomha, S. M.; Khalil, Kh. D.; El-Zanate, A. M.; Riyadh, S. M. *Heterocycles* **2013**, *87*, 1109-1120.
23. Gomha, S. M.; Ahmed, S. A.; Abdelhamid, A. O. *Molecules* **2015**, *20*, 1357-1376.

24. Novinson, T.; , R. M., Simon, L. N.; Robins, R. K.; Brien, D. E. *J. Med. Chem.***1974**, *17,* 645-648.

25. Cagniant P.; Caginate, D. *Adv. Heterocycl. Chem*. **1975**, *18,* 337- 482.

26. Bernier J. L.; Henichart, J. P. *J. Org Chem.* **1981**, *46*(*21*), 4197-4198.

27. Parr, R. W.; Reiss, J. A. *Aus. J. Chem*. **1984**, *37*, 1263-1270.

28. Kuecklander, U.; Huehnermann, W. *Arch. Pharm*. **1979**, *312(6)*, 515-526.

29. Card, A.; Caldwell, C.; Min, H.; Lokchander, B.; Hualin, X.; Sciabola, S.; Kamath, A. V.; Clugston, S. L.;Tschantz, W. R.; Leyu, W.; Moshinsky, D. J. *J. Biomol. Screen.***2009**, *14*, 31-42.

30. Perrin, D.; Fremaux, C.; Scheer, A. *J. Biomol. Screen.***2006**, *11*, 359-368.

31. Hopkins, A. L.; Groom, C. R.; Alex, A. *Drug Discovery Today*, **2004**, *9*, 430-431.

32. Smyth, L. A.; Collins, I. *J. Chem. Biol*. **2009,** *2*, 131-151.

33. Posy, S. L.; Hermsmeier, M. A.; Vaccaro, W.; Ott, K.; Todderud, G.; Lippy, J. S.; Trainor, G. L.; Loughney, D. A.; Johnson, S. R. *J. Med. Chem*. **2011**, *54*, 54-66.

34. Bamborough, P.; Brown, M. J.; Christopher, J. A.; Chung, C.; Mellor, G. W. *J. Med. Chem.* **2011**, *54*, 5131-5143.

35. Smyth, L. A.; Matthews, T. P.; Collins, I. *Bioorg. Med. Chem.* **2011**, *19*, 3569-3578.

36. Oza, V.; Ashwell, S.; Brassil, P.; Breed, J.; Ezhuthachan, J.; Deng, C.; Grondine, M.; Horn, C.; Liu, D.; Lyne, P.; Newcombe, N.; Pass, M.; Read, J.; Su, M.; Toader, D.; Yu, D.; Yu, Y.; Zabludoff, S. *Bioorg. Med. Chem. Lett.* **2012,** *22*, 2330-2337.

Figure captions:

Figure 1. Structures of some pyrrole and pyrazole scaffold-based biologically active PKIs.

Scheme 1. Synthesis of key synthons **2** and **3**.

Scheme 2. Synthesis of pyrazoles **7a-j** and pyrazolopyridazines **10a-f**.

Scheme 3. Synthesis of pyranone derivative **14**.

Scheme 4. Synthesis of compounds **16** and **18**.

Figure 2. 2D binding interactions of **7a** with active site amino acids of CHK1 (top panel); 3D binding interactions of **7a** (magenta-colored carbons) and the native ligand (cyan-colored carbons) with the active site amino acids of CHK1, hydrogen bonds are shown as orange lines (bottom panel).

Graphical Abstract

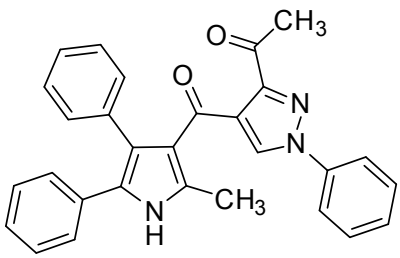

9a

CHK1 IC_{50} = 0.12 μM

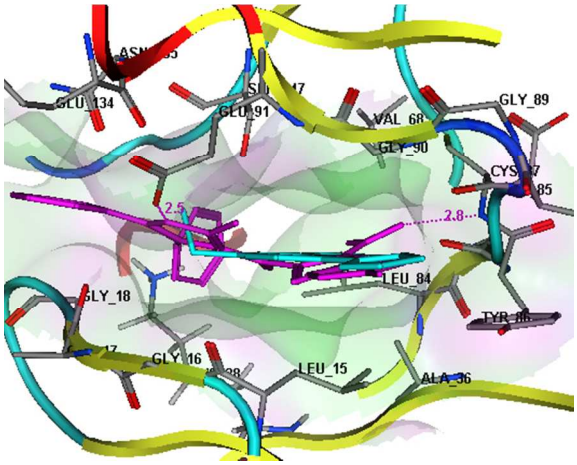

3D binding interactions of **7a** (magenta-colored carbons) and the co-crystallized ligand (cyan-colored carbons) with the active site amino acids of CHK1